Microbiological Research 228 (2019) 126301

Contents lists available at ScienceDirect

Microbiological Research

journal homepage: www.elsevier.com/locate/micres

Chumacin-1 and Chumacin-2 from *Pseudomonas aeruginosa* strain CGK-KS-1 as novel quorum sensing signaling inhibitors for biocontrol of bacterial blight of rice

Sirisha Kanugala[a,f], C. Ganesh Kumar[a,f,*], Rachamalla Hari Krishna Reddy[b], Babji Palakeeti[b], Kallaganti Venkata Siva Ramakrishna[c], Narendra Varma Nimmu[d], Cheemalamarri Chandrasekhar[a], Hitendra Kumar Patel[e], Thipparapu Ganapathi[g]

[a] Department of Organic Synthesis and Process Chemistry, CSIR-Indian Institute of Chemical Technology, Uppal Road, Tarnaka, Hyderabad 500007, India
[b] Department of Applied Biology, CSIR-Indian Institute of Chemical Technology, Uppal Road, Tarnaka, Hyderabad 500007, India
[c] Nuclear Magnetic Resonance Centre, CSIR-Indian Institute of Chemical Technology, Uppal Road, Tarnaka, Hyderabad 500007, India
[d] Department of Analytical Chemistry, CSIR-Indian Institute of Chemical Technology, Uppal Road, Tarnaka, Hyderabad 500007, India
[e] CSIR-Centre for Cellular and Molecular Biology, Uppal Road, Hyderabad 500007, India
[f] Academy of Scientific and Innovative Research, Ghaziabad 201002, India
[g] Stem Cell Research Division, Department of Biochemistry, ICMR-National Institute of Nutrition, Tarnaka, Hyderabad 500007, India

ARTICLE INFO

Keywords:
Quorum sensing
Diffusible signal factor
Bacterial blight
Biofilm
Xanthan gum

ABSTRACT

The *in vitro* inhibition of quorum sensing signal, xanthan gum secretion, biofilm formation in different *Xanthomonas* pathovars and biological control of bacterial blight of rice by the two bioactive extrolites produced by *Pseudomonas aeruginosa* strain CGK-KS-1 were explored. These extrolites were extracted from Diaion HP-20 resin with methanol and purified by preparative-thin layer chromatography. Further, spectroscopic structural elucidation revealed the tentative identity of these extrolites to be (*R*,3E,5E,9Z,11E)-13-((3*S*,5*R*)-5-acetyl-2,6-dimethylheptan-3-yl)-10-hydroxy-4-methyl-1,8-diazabicyclo[9.3.1]pentadeca-3,5,9,11(15),13-pentaen-2-one and (*R*,3E,5E,8E,11E)-13-((3*S*,5*R*)-5-acetyl-2,6-dimethylheptan-3-yl)-4-methyl-1,8-diazabicyclo[9.3.1]pentadeca-3,5,8,11(15),13-pentaene-2,10-dione, named as Chumacin-1 and Chumacin-2, respectively. Antimicrobial assay showed Chumacin-1 and Chumacin-2 exhibited a strong *in vitro* growth inhibition against various *Xanthomonas* pathovars. Quorum sensing overlay assay using a reporter strain *Chromobacterium violaceum* strain CV026 showed that Chumacin-1 and Chumacin-2 inhibited quorum sensing signaling. The mechanistic studies revealed that these extrolites inhibited the production of quorum sensing signaling factor, *cis*-11-methyl-2-dodecenoic acid; suppressed the xanthan gum secretion and also inhibited the biofilms formed by various *Xanthomonas* pathovars. Both Chumacin-1 and Chumacin-2 showed ROS generation in the test *Xanthomonas* strains, resulting in *in vitro* cell membrane damage was revealed through CSLM and FE-SEM micrographs. Further, greenhouse experiments using Samba Mashuri (BPT-5204) revealed that seed treatment with Chumacin-1 and Chumacin-2 along with foliar spray groups showed up to ~80% reduction in bacterial blight disease in rice. To the best of our knowledge, this is the first report on new quorum sensing inhibitors, Chumacin-1 and Chumacin-2 produced by *Pseudomonas aeruginosa* strain CGK-KS-1 exhibiting DSF inhibition activity in *Xanthomonas oryzae* pv. *oryzae*.

1. Introduction

Pathovars of the genus *Xanthomonas* are host specific and cause severe economic losses to various important agricultural crops by infecting a broad range of more than 390 crops (Ryan et al., 2011). The resistance of Xanthomonads towards conventional, synthetic chemical pesticides (Pernezny and Collins, 1997; Worthington et al., 2012; Richard et al., 2017), harmful effects of chemical pesticides, focus on environment and biodiversity protection have warranted the research to develop natural, ecofriendly and integrated pathogen control strategies including microbes as well as microbial derived bioactives for the control of plant pathogens (Hedin, 1982; Vidhyasekaran et al., 2001).

* Corresponding author.
E-mail addresses: cgkumar.iict@gov.in, cgkumar5@gmail.com (C.G. Kumar).

https://doi.org/10.1016/j.micres.2019.126301
Received 10 May 2019; Received in revised form 5 July 2019; Accepted 15 July 2019
Available online 20 July 2019

Conventional chemical eradication of plant pathogens aims at killing or inhibiting their growth but fails to break bacterial communication system, the key for resistance acquisition. The bacterial cells secrete an exopolysaccharide matrix, colonize, and form biofilm inside the host. The pathogenic bacteria also employ cell-cell communication network to acquire resistance towards antimicrobials and chemicals to make an edge over competing microbial populations. This intercellular communication or quorum sensing confers pathogenic bacteria with selective advantage over competitor microbes, host immune evasion, resistance to pesticides, detergents, disinfectants, antimicrobials, antibiotics, etc. Moreover, the over-usage of antimicrobial chemicals poses an intense selection pressure on the pathogenic bacteria, leading to evolution of more resistant bacteria. Hence, there is a serious need for the exploration of novel control strategies that can break the bacterial quorum and that could act as quorum sensing inhibitors. Xanthomonads operate their cell-cell communication system by a chemical signal, which is *cis*-11-methyl dodecenoic acid, called diffusible signal factor (DSF). This DSF signaling has been shown to regulate the physiological and social behavioral traits of the Xanthomonads, like chemotaxis, motility, EPS secretion, colonization, biofilm formation, iron uptake and pathogenicity to plant hosts. DSF is synthesized by an enzyme, DSF synthase, coded by the gene *rpfF* (regulation of pathogenicity factor F). Thus quorum sensing and the *rpfF* gene products form an attractive target for effective control of Xanthomonads (Ryan et al., 2015).

Microbial bioactive compounds of natural origin, with their innate ability to overcome the competing bacterial communication system by breaking their quorum signaling, along with innate antagonism for plant pathogens and biodegradable nature makes them an excellent choice for their use as ecofriendly agrochemicals. Among microbes, Pseudomonads exhibited a strong antagonism towards a broad spectrum of plant pathogens, which could be deciphered from studies carried out using various *Pseudomonas* strains and their secondary metabolites as natural bactericides and fungicides (Pernezny and Collins, 1997; Mazurier et al., 2009; Takeuchi et al., 2015; Bernal et al., 2017). Among the *Pseudomonas* strains, *P. fluorescens* strain G-92 (Expert and Digat, 1995), *P. putida* strain T1-5 (Expert and Digat, 1995), *P. aeruginosa* strain NJ-15 (Bano and Musarrat, 2003), *P. chlororaphis* strain PCL 1391 (Chin-A-Woeng et al., 2000), were reported to exhibit biocontrol properties. Many bioactive compounds including 2,4-diacetylphloroglucinol (Lanteigne et al., 2012), pyoluteorin (Ramette et al., 2011), HCN (Lanteigne et al., 2012), non-ribosomal peptides (Michelsen et al., 2015), phenazines (Chin-A-Woeng et al., 2003), volatile organic compounds (Raza et al., 2016), biosurfactants (Debode et al., 2007), cyclic lipopeptides (Raaijmakers et al., 2006), etc. produced by different species and strains of genus *Pseudomonas* play a functional role as promising antagonists against plant pathogens.

In the present study, we screened crude extracts solubilized in DMSO for 1340 bacterial strains available as in-house departmental culture collection for their antimicrobial potential against a panel of *Xanthomonas* pathovars by agar well diffusion method. The strain ICTB-315 showed promising activity and it was identified by 16S rRNA sequencing as *Pseudomonas aeruginosa* strain CGK-KS-1 (GenBank Accession No. KY203649). The metabolic profiling of the methanolic crude extract extracted from Diaion HP-20 resin by TLC has revealed four bands. The bioactivity guided fractionation has reaveled two major bioactive bands and two minor bands in the crude extract. The major bioactive bands were structurally elucidated using various spectroscopic techniques. These two major bioactive extrolites, E-1 and E-2 produced by strain CGK-KS-1 effectively suppressed the growth of various *Xanthomonas* strains. The anti-*Xanthomonas* mechanism of these bioactive compounds was demonstrated through various studies including ROS generation, membrane disruption, biofilm destruction, inhibition of quorum sensing signal, DSF and suppression of xanthan gum production. HPLC and HRMS studies indicated the suppression of DSF signal by E-1 and E-2 treatment in *X. oryzae* pv. *oryzae* strain TNAU-2. These studies were further confirmed by greenhouse studies with these bioactive compounds which revealed their promising ability to suppress the development of bacterial blight in rice caused by *X. oryzae* pv. *oryzae* strain TNAU-2. Molecular docking studies also showed that the bioactive extrolites E-1 and E-2 could strongly interact with the protein pocket of DSF synthase, *rpfF*. This study reports for the first time the quorum sensing inhibition, xanthan gum supression, biofilm disruption in Xanthomonads exhibited by the bioactive extrolites produced by strain CGK-KS-1.

2. Materials and methods

2.1. Microorganism, fermentation conditions, extraction and TLC bioautography of extrolites

Strain CGK-KS-1 was cultured aerobically in Luria-Bertani medium (pH 7.0 ± 0.2) at 32 °C with agitation at 150 rpm for 2 days in an orbital shaker (New Brunswick Scientific, Edison, NJ, USA). This was used as seed culture to inoculate the production medium in the bioreactor. The production of bioactive extrolites from the strain CGK-KS-1 was carried out under sterile aerobic conditions for 72 h in a 5 L Biostat B Plus double jacketed glass bioreactor (Sartorius Stedium Biotech, Göttingen, Germany) supported by a Rushton type impeller and interfaced with a turbidostat probe. Batch fermentation was carried out using a production medium (3 L working volume) comprised of Luria Bertani broth (pH 7.0) under optimized conditions of inoculum (0.1%), temperature of 32 °C, air flow of 0.1 vvm and agitation rate of 150 rpm. Silicone oil was used as an antifoam agent. A total of ten fermentation batches were run in the bioreactor. The fermented medium was subjected to centrifugation at 8500 × *g* for 20 min at room temperature to obtain the cell-free supernatant. The bioactive compounds from the cell-free supernatant were adsorbed onto the resin (Diaion HP-20, 3% (w/v), Supelco, Bellafonte, PA), followed by extraction with methanol. The recovered methanolic crude extract was dried by rotaevaporation and subjected to thin-layer chromatography on silica gel 60 TLC plates (F_{254}, Merck), using a solvent system of methanol-chloroform (5:95) to reveal the metabolic profile when observed under UV light at 254 nm in a TLC Cabinet 4 (CAMAG, Wilmington, NC, USA). The resolved TLC plates were further used for TLC bioautography against various strains and species of *Xanthomonas* pathovars (Choma and Grzelak, 2011).

2.2. Purification and structural characterization

The crude extract was used for purification by preparative-TLC using 1 mm thick silica gel 60 (F_{254}, Merck) TLC plates, using solvent system of methanol-chloroform (5:95) as a mobile phase. The resolved fractions corresponding to R_f values of 0.52 and 0.67 were collected in methanol, filtered through 0.22 µm nylon syringe filters (Millex-HN, Millipore) and subjected to drying under vacuum with rotary evaporation (Rotavapor R-205, Büchi, Switzerland). The absorbance under UV and visible regions of the purified extrolites, E-1 and E-2 were measured with a UV–vis spectrophotometer (Lambda 25, Perkin-Elmer, Shelton, CT). The purity of the bioactive compounds were assessed by HPLC (Shimadzu, Japan, Phenomenex reverse phase C18 column, 4.6 × 150 mm length and 5 µm width) using mobile phase of Milli Q water and acetonitrile (98:2, v/v) along with 0.1% acetic acid. The pure extrolites, E-1 and E-2 were analyzed by various spectroscopic techniques, namely NMR, FT-IR, and MS to assess their structure. The spectras of ^{1}H NMR, ^{13}C NMR, 2D-NMR including ^{1}H-$^{1}H-COSY$, NOESY, TOCSY, HSQC, HMBC in $CDCl_3$ were recorded on Bruker Avance 300 MHz NMR spectrometer (Bruker, Switzerland). The corresponding chemical shifts are represented in ppm and tetramethylsilane served as control. The molecular weights of the bioactive compounds were determined using QSTAR XL Hybrid ESI-Q TOF mass spectrometer (Applied Biosystems Inc., Fosters City, CA, USA). The functional groups of the bioactive compounds were assessed as KBr pellets using Thermo-

Nicolet Nexus 670 FT-IR spectrophotometer (ThermoFisher Scientific Inc., Madison, WI, USA), in the wavenumber range of 400-4,000 cm^{-1}. The UV absorbance was recorded in methanol at a wavelength range of 190–700 nm to check the absorbance maxima of the pure extrolites.

2.3. Antimicrobial activity

The pure extrolites were tested for *in vitro Xanthomonas* inhibition activity by agar well diffusion method (Amsterdam, 1996). The various pathogenic *Xanthomonas* strains namely, *X. oryzae* pv. *oryzae* strain BXO43, *X. oryzae* pv. *oryzae* strain TNAU-2, *X. oryzae* pv. *oryzicola* strain Y2, *X. campestris* pv. *vesicatoria* strain XIS, *X. campestris* pv. *vesicatoria* strain 65-10, *X. campestris* pv. *vesicatoria* strain 85-10, *X. campestris* pv. *vesicatoria* strain 8004, *X. campestris* pv. *campestris* strain C1, *X. campestris* pv. *campestris* strain TNAU-1, *X. campestris* pv. *campestris* MTCC 2286, *X. axonopodis* pv. *malvacaerum* strain TNAU-3 were cultured in sucrose-peptone broth comprising of sucrose 1% (w/v) and bacteriological peptone 1% (w/v) at 30 °C for 24 h with agitation at 150 rpm. *Chromobacterium violaceum* strain CV026 was grown in Luria Bertani broth supplemented with kanamycin at 28 °C for 24 h with agitation at 150 rpm. The test strains of an inoculum concentration of 10^6 cfu/ml (0.5 McFarland standard) were seeded separately onto sucrose-peptone agar plates. Wells were prepared in the agar and loaded with the pure extrolites at a dose range of 0–125 µg/mL. Copper oxychloride ($Cu_2(OH)_3Cl$, 0–125 µg/mL) and DMSO were run in parallel as positive and negative controls, respectively. The assay was performed in triplicates and the Minimum Inhibitory Concentration (MIC) values of the test compounds were determined from the mean of triplicates. The well containing the least concentration of the pure extrolite exhibiting an inhibition zone was considered as the MIC value of the corresponding test compound.

2.4. Quorum sensing inhibition assay

Chromobacterium violaceum strain CV026 (CV026), a double mini-Tn5 mutant that lacks DSF expression and violacein pigmentation, was used as a reporter strain (Zhu et al., 2011) to monitor quorum-sensing inhibition by the pure extrolites, E-1 and E-2 derived from the strain CGK-KS-1. External DSF supplementation restored the quorum sensing signaling and violacein pigmentation of CV026 mutant strain. In this assay, the strain CV026 was cultured in kanamycin-supplemented Luria-Bertani (LB) broth at 28 °C with agitation at 150 rpm. An inoculum density of 10^6 cfu/mL (equivalent to 0.5 McFarland standard) of CV026 strain was mixed with molten agar and surface plated as a thin layer onto the LB agar plates. The wells were prepared with a cork borer and loaded with commercial *cis*-11-methyl-2-dodecenoic acid (DSF derived from *Xanthomonas campestris*; CAS No. 677354-23-3; Sigma Chemical Co., St Louis, MO, USA), pure extrolites (E-1) and (E-2) [MIC value of 3.9 µg/mL (9.39 µM) and 3.9 µg/mL (9.42 µM), respectively], commercial DSF (100 µg/mL) + extrolite E-1 [3.9 µg/mL (9.39 µM)], commercial DSF (100 µg/mL) + extrolite E-2 [3.9 µg/mL (9.42 µM)] and control PBS, separately. These plates were incubated overnight to observe the effect of E-1 and E-2 on quorum sensing signaling mechanism. Triplicates of the experiments were carried out with strain CV026 to assess the quorum sensing inhibition property of the pure extrolites. In all the experimental groups, DSF was added at a concentration of 100 µg/mL, which was the optimized concentration obtained from the DSF-overlay assay with *Chromobacterium violaceum* strain CV026 (data not shown).

2.5. Xanthan gum extraction and quantification

Members of genus *Xanthomonas* secrete very high amounts of EPS called xanthan gum. This gum forms a strong, viscous supporting matrix or a biofilm which accumulates in the vascular system of rice plants leading to necrosis and cell death of plant cells. This EPS also acts as a protective shield to prevent external shocks like chemicals and plant immune mechanisms (He and Zhang, 2008). In this context, it is warranted to search for novel bioactives that could suppress xanthan gum production. In the present study, the effect of pure extrolites E-1 and E-2 at a concentration of 3.9 µg/mL (9.39 µM) and 3.9 µg/mL (9.42 µM), respectively, was assessed for the quantity of xanthan gum secreted by *X. campestris* pv. *campestris* MTCC 2286, a prolific producer of xanthan gum. Briefly, the MTCC 2286 culture was grown in 250 mL of sucrose-peptone broth at 30 °C for 24 h with agitation at 200 rpm. Then the culture was treated with pure extrolites E-1 and E-2 and then allowed to ferment for an additional 24 h. In parallel, the untreated culture was used as control. After incubation, the cell-free supernatant was collected, 1% KCl (w/v) was added and stirred for 2 h. The produced xanthan gum was precipitated with isopropanol followed by quantification of the precipitated xanthan gum (Flahive et al., 1994).

2.6. Biofilm inhibition activity

Biofilms are specialized consortia of bacterial cells living together in a matrix composed of lipopolysaccharides, DNA, peptides, etc. These biofilm matrices help members of *Xanthomonas* pathovars in developing resistance towards antibiotics and chemicals, owing to the complexity of the xanthan gum and other matrix substances (Flemming and Wingender, 2010; Worthington et al., 2012). The ability of the pure extrolites, E-1 and E-2 derived from the strain CGK-KS-1 to inhibit biofilm formation by *Xanthomonas* pathovars and CV026 was assessed by crystal-violet microtiter plates (Christensen et al., 1985). Briefly, the panel of *Xanthomonas* pathovars were cultured in sucrose-peptone broth at 30 °C for 48 h without shaking to support biofilm development. Strain CV026 was grown in Luria-Bertani broth supplemented with kanamycin at 28 °C for 48 h without shaking. The biofilms were later treated with E-1 at a dose of 0, 2, 4, 8, 16 and 20 µg mL^{-1} (0, 4.83, 9.66, 19.32, 38.64 and 48.30 µM) and E-2 at a dose of 0, 2, 4, 8, 16 and 20 µg mL^{-1} (0, 4.84, 9.68, 19.37, 38.74 and 48.72 µM) for 24 h. PBS washing was employed for removal of unanchored cells and retention of biofilm on the walls of the microtiter plates. These biofilms were stained with crystal violet (0.1%) for 45 min at room temperature. Excess stain was washed off and the crystal violet stained *Xanthomonas* biofilms were dried overnight and solubilized in 90% ethanol. The biofilms were quantified by measuring their absorbance using Infinite M200Pro plate reader (Tecan Group Ltd., Mannedörf, Switzerland) at 540 nm. The biofilm inhibitory concentrations in terms of IC_{50} values (in µM) were deduced from the corresponding $A_{540\ nm}$. All the biofilm experiments were performed in triplicates and the mean values are represented with standard deviations.

2.7. Field emission scanning electron microscopy (FE-SEM) and biofilm disruption

The biofilm inhibition potential of the pure extrolites was investigated against the biofilm formation by *X. oryzae* pv. *oryzae* strain TNAU-2. *Xanthomonas* cells were cultured at 30 °C for 48 h in sucrose-peptone broth to allow biofilm formation. Later the biofilms were treated with the pure extrolites, E-1 [3.9 µg/mL (9.39 µM)] and E-2 [3.9 µg/mL (9.42 µM)] for 3 h. The untreated *Xanthomonas* cells served as control group. The cells were washed and fixed with glutaraldehyde in PBS buffer. This was followed by serial washings with ethanol gradients of 10%, 30%, 50%, 70% and 100%. The fixed cells were allowed to dry and then sputtered with gold-palladium coating onto the cover slips for visualization under JSM 7610 F Schottky Field Emission Scanning Electron Microscope (JEOL USA Inc., MA, USA) operated at accelerating voltage of 100 kV (Soboh et al., 1995).

2.8. Confocal scanning laser microscopy (CSLM) for assessing cell membrane integrity

Cell membrane is a crucial component of any bacterial cell as it acts as a primary and strong drug barrier to the cell that plays a major role in drug resistance development (Hancock, 1997). The effect of the pure extrolites, E-1 [3.9 µg/mL (9.39 µM)] and E-2 [3.9 µg/mL (9.42 µM)] was assessed for cell membrane integrity of the *X. oryzae* pv. *oryzae* strain TNAU-2 by CSLM using LIVE/DEAD® *Bac*Light™ Bacterial Viability Kit (Molecular Probes Inc., Eugene, OR, USA). This kit comprises of two fluorescent dyes, SYTO 9 and propidium iodide. SYTO 9, a green fluorescent nucleic acid dye which is permeable to live cells of *X. oryzae* pv. *oryzae* with an intact membrane that stains the live cells green when visualized under a confocal microscope. While, propidium iodide stains only those cells with damaged membranes which indicates whether the cells were dead or going to be dead due to the cell membrane damage. Briefly, the 24 h fresh *Xanthomonas* cells were treated with the pure extrolites for 3 h, while the untreated *Xanthomonas* cells served as control. Both the groups were subjected to staining with SYTO 9 and propidium iodide, fixed in 0.1% formaldehyde and then visualized under Eclipse Ti confocal laser scanning microscope (Nikon Corporation, Tokyo, Japan) with 480–490 nm argon ion laser for excitation and emission at 500–635 nm band pass filter. The Ti Control ver. 4.4.4 software interfaced with the CSLM was used for image processing with the scale bar for each image of 10 µm.

2.9. Intracellular ROS quantification

The mode of action of the pure extrolites, E-1 [3.9 µg/mL (9.39 µM)] and E-2 [3.9 µg/mL (9.42 µM)] on the susceptible *Xanthomonas* strains was studied by measuring the intracellular generated ROS if any, by NBT based assay. All the *Xanthomonas* strains were cultured in sucrose-peptone broth at 30 °C for 48 h with agitation at 150 rpm. The *Xanthomonas* cultures were adjusted to an optical density equivalent to 10^6 cfu/ml (0.5 McFarland standard). These strains were loaded into the wells of 96 well microtitre plate and treated with extrolites, E-1 [3.9 µg/mL (9.39 µM)] and E-2 [3.9 µg/mL, (9.42 µM)] for 3 h. The untreated strains served as control groups. After incubation, all the groups were treated with 0.1% NBT in PBS at room temperature and left undisturbed for 45 min. The absorbances of all the *Xanthomonas* groups were recorded at 540 nm. The *Xanthomonas* strains vs. their corresponding absorbances at 540 nm were plotted. All the experiments were carried out in triplicates and the mean values were used for deriving the standard deviations.

2.10. Diffusible signal factor (DSF) extraction, detection and quantification

Diffusible signal factor (DSF) secreted by *X. oryzae* pv. *oryzae* strain TNAU-2 was extracted by the method as reported (Zhou et al., 2017). *X. oryzae* pv. *oryzae* strain TNAU-2 was cultured in the sucrose-peptone broth at 30 °C for 48 h and this culture was treated overnight for 12 h with the pure extrolites, E-1 [3.9 µg/mL (9.39 µM)] and E-2 [3.9 µg/mL (9.42 µM)] at 30 °C with agitation at 150 rpm. The untreated group was run in parallel as control. After this treatment, the broth was centrifuged at 5000 rpm and 4 °C and the supernatant was mixed with ethyl acetate, followed by pH adjustment to 4.0. The acidified extract was concentrated by rotary evaporation and further dissolved in HPLC grade methanol. The presence of DSF in the methanol fractions were detected on Shimadzu HPLC interfaced with a UV detector employing a Luna Reverse phase C18 column (4.6 × 150 mm length and 5 µm width) by isocratic elution using solvent system of water-methanol (80:20) at a flow rate of 1 ml/min. The molecular mass of the extracted DSF was also confirmed by high resolution mass spectrometry.

2.11. Greenhouse experiments

The control of bacterial blight of rice caused by *X. oryzae* pv. *oryzae* strain TNAU-2 was evaluated by treatment of husked rice seeds with the pure extrolites, E-1 and E-2. The pure extrolites in the concentration range of 25 mg, 50 mg, 100 mg and 200 mg in 2 mL methanol each were mixed with 98 mL of sterile distilled water saturated with 200 µl/mL of Tween-20. The final concentrations of 250 µg/mL, 500 µg/mL, 1000 µg/mL and 2000 µg/mL were used for the treatment of seeds of rice cultivar, Samba Mashuri (BPT-5204) for 24 h. In case of experimental control, the seeds were treated with commercial agrochemical, copper oxychloride. *X. oryzae* pv. *oryzae* strain TNAU-2 was cultured on sucrose-peptone agar at 28 °C for 48 h. The cells were washed thrice with sterile distilled water, and an inoculum density of 0.1 $OD_{600\ nm}$ (10^6 cfu/ml) was used for infecting the three week old rice plants germinated after seed treatment (Vidhyasekaran et al., 2001). Following seed treatment, copper oxychloride treated plants and uninfected plants were used as positive and negative controls. After infection with TNAU-2 strain by leaf clipping, the plants were foliar sprayed with 1000 µg/mL of the two pure extrolites and copper oxychloride (control) at periodic interval of 5 days for up to 45 days (Sinha et al., 2013). All the plants were maintained under greenhouse conditions of 70–80% relative humidity (RH) and 30 °C. The bacterial migration through vascular routes and through the leaf blade was evaluated by bacterial leaf migration assay (Dharmapuri and Sonti, 1999). After 15 days of infection, the leaves from the control and treated groups were collected and cut into 1.2 cm pieces. These leaf pieces were layered over the sucrose peptone agar plates supplemented with antifungal drug, miconazole (to prevent fungal contamination). The plates were incubated for 48 h to observe the presence or absence of *Xanthomonas* strain in the xanthan gum oozed out from the cut edges of the leaves.

2.12. Molecular docking studies

Docking studies were performed to identify the interactions of the two pure extrolites, E-1 and E-2 with the crystal structure of *RpfF*, which is a diffusible signal factor synthase of *X. campestris* pv. *campestris* (PDB ID: 3M6N) using Molegro Virtual Docker (installed on an Intel Centrino Machine, Intel Corporation, Santa Clara, CA, USA). All the ligand structures were constructed using Chem3D Ultra 8.0 software, and then these structures were energetically minimized by using MOPAC (semi-empirical quantum mechanics), Jop Type with 100 iterations and minimum RMS gradient of 0.01, and saved as protein data bank (.pdb) format.

2.13. Statistical analysis

All the experiments were performed in triplicates and the results were presented as mean ± standard error of mean. One-way ANOVA was used to analyze the data by using GraphPad PRISM version 6.0 (GraphPad Software, Inc, La Jolla, CA, USA). The resulting values with $P < 0.05$ were taken as significant.

3. Results and discussion

3.1. Characterization and structural elucidation of the bioactive extrolites

The present study emphasizes on extrolites produced by *Pseudomonas aeruginosa* strain CGK-KS-1 having the ability to inhibit quorum sensing mediated DSF secretion, xanthan production and biofilm formation, which impart virulence in diverse pathovars of genus *Xanthomonas*, the causative agents for bacterial blight diseases in different agriculturally important crops. The crude methanolic extract from strain CGK-KS-1 on TLC plate showed four spots which were UV active at 254 nm. These two major spots could also be visualized when stained with iodine. Further, the crude TLC autobiography assay on

agar plates seeded with various *Xanthomonas* pathovars revealed two zones of inhibition for the major spots corresponding to R_f values of 0.52 and 0.67, respectively, while the minor spots showed no antimicrobial activity. The metabolite profiling by TLC and bioactivity guided fractionation showed that the bioactive extrolites E-1 and E-2 were produced at an approximate amounts of 0.7 ± 0.01 g/L and 0.6 ± 0.01 g/L, respectively, while the two minor fractions accounted to 0.1 g/L and 0.15 g/L, respectively; while the total crude exrtact obtained was 1.55 ± 0.01 g/L (averaged from 10 fermenter batches). These two major extrolites were further purified and on HPLC analysis they showed 97% purity with retention times of 2.665 min and 2.660 min, respectively (Supplementary Figs. S1a and S1b). Both these extrolites were yellowish in colour, partially sticky and were soluble in different organic solvents including methanol, acetone, ethanol, ethyl acetate, hexane, dimethyl sulfoxide, chloroform and sparingly soluble in water. The elemental composition of pure extrolites E-1 and E-2 is depicted in Supplementary Table S1. The melting points of E-1 and E-2 were 252 °C and 257 °C, respectively. The λ_{max} recorded in methanol for both these pure extrolites was 254 nm (Supplementary Figs. S2a and S2b). The FT-IR spectral data for both these extrolites are represented in Supplementary Table S2.

The ^{1}H NMR of extrolite E-1 (Supplementary Fig. S3) showed the following chemical shifts (δ, ppm): ^{1}H NMR (500 MHz, $CDCl_3$): δ 0.88-0.99 (m, 12 H), 1.0–1.25 (m, 1 H), 1.41–1.90 (m, 3 H), 2.02–2.04 (m, 1 H), 2.17 (s, 3 H), 2.32–2.33 (m, 1 H), 2.79–3.39 (m, 2 H), 3.51 (d, 1 H), 3.97 (dd, 2 H), 4.00 (dd, 1 H), 5.86 (s, 1 H), 6.22 (s, 1 H), 7.23 (d, 1 H), 7.29 (m, 1 H), 7.35 (m, 1 H), 7.49 (m, 1 H), 8.30 (m, 1 H) ppm. The ^{13}C NMR spectra of extrolite E-1 showed well resolved aromatic carbons and aliphatic carbons as shown in the Supplementary Table S3 and the ^{13}C NMR spectra are shown as Fig. 1a and b. The chemical shifts at 53.61, 56.42, 59.32, 60.70 and 61.75 ppm corresponded to CH—NH stretch of E-1. The peaks at 129.36, 123.60, 127.46 ppm represent aromatic carbons of E-1. The ^{1}H-^{1}H COSY spectrum of E-1 (Supplementary Fig. S4) also gave a correlation of proton assignments in the ^{1}H NMR spectra for both these extrolites. The NOESY spectrum (Supplementary Fig. S5) showed a representation of the closely placed non-bonded protons in E-1. The ESI-MS of extrolite E-1 is shown in Supplementary Fig. S6. Based on ESI-MS (m/z) spectral analysis, the calculated mass for E-1 is 414 $[M+H]^+$ and molecular formula is $C_{25}H_{36}N_2O_3$. The corresponding HR—MS spectra of E-1 is shown as Supplementary Fig. S7.

The ^{1}H NMR of extrolite E-2 (Supplementary Fig. S8) showed the following chemical shifts (δ, ppm): ^{1}H NMR (500 MHz, CDCl3): δ 0.87-0.99 (m, 12 H), 1.07–1.64 (m, 4 H), 1.78–1.91 (m, 2 H), 2.04–2.06 (m, 1 H), 2.32-2.91(m, 3 H), 3.52 (d, 1 H), 3.94 (d, 1 H), 4.08 (d, 1 H), 4.36 (d, 1 H), 6.18 (d, 1 H), 7.23 (m, 1 H), 7.24 (m, 1 H), 7.27–7.35 (m, 1 H) ppm. The ^{13}C NMR spectra of E-2 showed well resolved aromatic carbons and aliphatic carbons as shown in the Supplementary Table S3. In the ^{13}C NMR spectra The chemical shifts at 53.43, 56.25, 59.02, 60.53, 61.79 ppm attributed to CH—NH stretch of E-2, while the peaks at 129.02, 123.42, 127.71 ppm represent aromatic carbons of E-2. The ^{1}H-^{1}H COSY spectrum of E-2 (Supplementary Fig. S9). The NOESY spectrum of E-2 (Supplementary Fig. S10) showed a representation of the closely placed non-bonded protons. The ESI-MS of the E-2 is shown in Supplementary Fig. S11. Based on ESI-MS (m/z) spectral analysis, the calculated mass for E-2 is 413 $[M+H]^+$, molecular formula is $C_{25}H_{35}N_2O_3$. The corresponding HR—MS spectra of E-2 is shown as Supplementary Fig. S12.

Based on ^{1}H and ^{13}C NMR, 2D NMR, FT-IR and MS spectral analysis, E-1 and E-2 produced by *P. aeruginosa* strain CGK-KS-1 were tentatively identified as (*R*,3E,5E,9Z,11E)-13-((3*S*,5*R*)-5-acetyl-2,6-dimethylheptan-3-yl)-10-hydroxy-4-methyl-1,8-diazabicyclo[9.3.1]pentadeca-3,5,9,11(15),13-pentaen-2-one and (*R*,3E,5E,8E,11E)-13-((3*S*,5*R*)-5-acetyl-2,6-dimethylheptan-3-yl)-4-methyl-1,8-diazabicyclo [9.3.1]pentadeca-3,5,8,11(15),13-pentaene-2,10-dione, respectively. Both these pure extrolites, E-1 and E-2, were named as Chumacin-1 and Chumacin-2 (*Etymology*: Chuma- derived from Chumathang hot spring, Ladakh, a place from where the soil sample was collected, -cin represents antimicrobial activity).

3.2. Antimicrobial activity

The *in vitro* antimicrobial activity of Chumacin-1 and Chumacin-2 against different species and strains of *Xanthomonas* pathovars was performed by agar well diffusion assay and the results to this regard are depicted in Table 1. Chumacin-1 exhibited a broad spectrum antimicrobial activity against all the tested *Xanthomonas* pathovars. It showed promising inhibitory activity against *X. oryzae* pv. *oryzae* strain TNAU-2, *X. oryzae* pv. *oryzicola* stain Y2, *X. campestris* pv. *vesicatoria* strain XIS, *X. campestris* pv. *vesicatoria* strain 65-10, *X. campestris* pv. *campestris* strain TNAU-1 and *Chromobacterium violaceum* strain CV026 at a minimum inhibitory concentration of 3.9 μg/mL (9.39 μM). Chumacin-1 showed good inhibition of *X. campestris* pv. *vesicatoria* strain 85-10 and *X. campestris* pv. *vesicatoria* strain 8004 at a minimum inhibitory concentration of 7.8 μg/mL (18.78 μM). While, Chumacin-2 showed promising inhibition against *X. oryzae* pv. *oryzae* strain TNAU-2, *X. oryzae* pv. *oryzicola* strain Y2, *X. campestris* pv. *vesicatoria* strain 65-10, *X. campestris* pv. *campestris* strain TNAU-1, *X. campestris* pv. *campestris* MTCC 2286, *Chromobacterium violaceum* strain CV026 and *X. campestris* pv. *vesicatoria* strain 85-10 at a minimum inhibitory concentration of 3.9 μg/mL (9.42 μM), while it exhibited good inhibition against *X. campestris* pv. *vesicatoria* strain XIS and *X. campestris* pv. *vesicatoria* strain 8004 at a minimum inhibitory concentration of 7.8 μg/mL (18.84 μM). While the tested *Xanthomonas* pathovars were highly resistant (MIC value of 62.5 μg/mL) to the commercial agrochemical, copper oxychloride (control). The MIC values exhibited by Chumacin-1 and Chumacin-2 against various *Xanthomonas* strains were very much lower than the reported bioactive compounds from earlier literature including benzoic acid (MIC value: 48 μg/mL) and phenylacetic acid (MIC value: 10 μg/mL) derived from *Pseudomonas aeruginosa* SRM1 2 (Kulshreshtha and Velusamy, 2012), synthetic compounds such as niclosamide (MIC value: 4.2 μg/mL) and auranofin (MIC value: 5 μg/mL) as reported by Kim et al. (2016) and bioactive fraction, F3 (MIC value: 100 μg/mL) derived from *Pseudomonas* sp. LV strain (Munhoz et al., 2017).

3.3. Quorum sensing inhibition assay

Members of genus *Xanthomonas* produce a diffusible signal factor (DSF) identified as *cis*-11-methyl-2-dodecenoic acid, which is part of the intracellular signaling system that allows the bacterial population to monitor their cell density. This property of the bacteria to sense the population density is termed as quorum sensing (QS), which includes gene mediated phenotypic expression of various virulence factors like xanthan gum (EPS), extracellular enzymes, siderophores, etc., which collectively are essential for virulence or pathogenicity of *Xanthomonas* pathovars (Dong et al., 2001). Quorum sensing is a cell density and signal factor concentration dependant communication system that enables a bacterial cell to sense, compete and survive in its natural habitat comprising of neighbouring microbial members from intraspecies and interspecies. Especially, quorum sensing helps bacteria to behave in a well regulated synchrony as a response to inhabiting environmental conditions like nutrient availabilty, competition with other microbes, defending from other microbial cells, chemicals, toxins and evading the host immune system. In the context of complex and intricate co-existence of diverse microbial communities together, there might be a possibility of different bacteria using common chemical signals or chemical language. This implies that bacteria from different species may secrete and respond to the similar or identical chemical signals in a quorum sensing cross talk (Ferluga et al., 2008; Silva Vasconcellos et al., 2014). A single bacterial species could have more than one quorum sensing system and could respond to more than one chemical

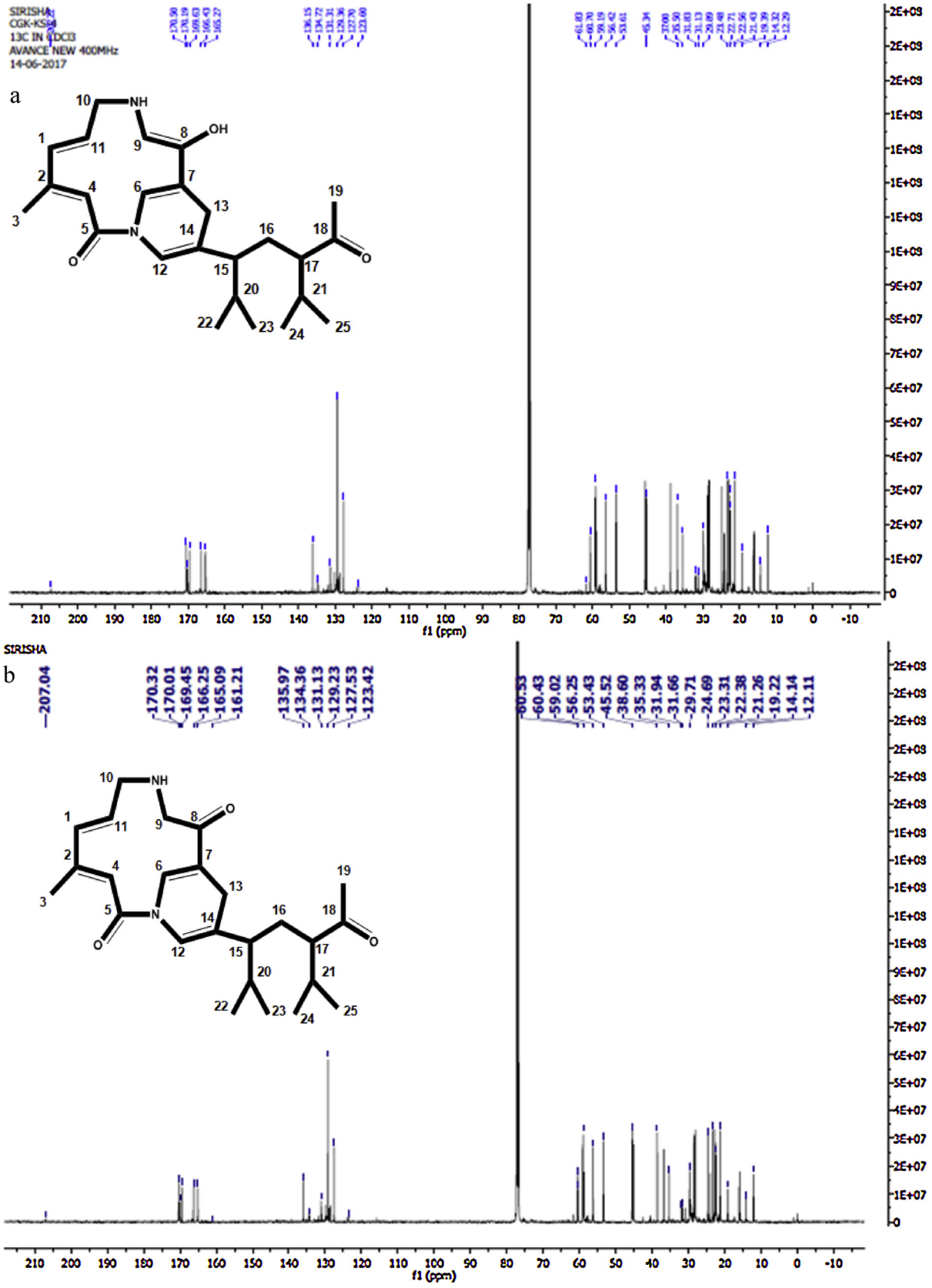

Fig. 1. (a)^{13}C NMR spectrum of pure extrolite, E-1 from *Pseudomonas aeruginosa* CGK-KS-1. (b) ^{13}C NMR spectrum of pure extrolite, E-2 from *Pseudomonas aeruginosa* CGK-KS-1.

Table 1
Antimicrobial activity of Chumacin-1 and Chumacin-2 against different species and strains of *Xanthomonas* pathovars.

Test pathogens	Chumacin-1		Chumacin-2		Copper oxychloride		Tetracycline	
	MIC[†]	MBC[‡]	MIC[†]	MBC[‡]	MIC[†]	MBC[‡]	MIC[†]	MBC[‡]
X. oryzae pv. *oryzae* strain BXO43	15.6	32.5	15.6	32.5	125	250	–	–
X. oryzae pv. *oryzae* strain TNAU-2	3.9	7.8	3.9	7.8	62.5	125	–	–
X. oryzae pv. *oryzicola* strain Y2	3.9	7.8	3.9	7.8	62.5	125	–	–
X. campestris pv. *vesicatoria* strain XIS	3.9	7.8	7.8	15.6	62.5	125	–	–
X. campestris pv. *vesicatoria* strain 65-10	3.9	7.8	3.9	7.8	62.5	125	–	–
X. campestris pv. *vesicatoria* strain 85-10	7.8	15.6	3.9	15.6	125	250	–	–
X. campestris pv. *vesicatoria* strain 8004	7.8	7.8	7.8	7.8	125	250	–	–
X. campestris pv. *campestris* strain C1	15.6	32.5	15.6	32.5	125	250	–	–
X. campestris pv. *campestris* strain TNAU-1	3.9	7.8	3.9	7.8	125	250	–	–
X. campestris pv. *campestris* MTCC 2286	3.9	7.8	3.9	7.8	62.5	125	–	–
X. axonopodis. pv. *malvacerum* strain TNAU-3	–	–	–	–	62.5	125	–	–
Chromobacterium violaceum strain CV026	3.9	7.8	3.9	7.8	–	–	1.9	3.9

[†]MIC: Minimum Inhibitory Concentration- The least concentration of a test compound which inhibits visible growth of test microorganism.
[‡]MBC: Minimal bactericidal concentration is the dose of an antibacterial agent required to kill a particular test microorganism. (MIC and MBC values are represented in μg/mL at $P < 0.05$).

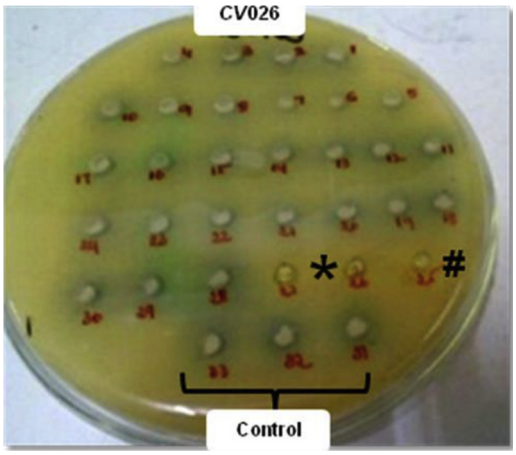

Fig. 2. Quorum sensing overlay assay to evaluate violacein pigment production by *Chromobacterium violaceum* strain CV026 (double mini-Tn5 mutant). All the wells were loaded with various concentrations of Chumacin-1 and Chumacin-2, except the control wells. In the overlay assay of strain CV026 onto LB agar, wells loaded with Chumacin-1 and Chumacin-2 at dose less than their MIC, showed the pigmentation. Whereas the well lacking pigmentation, labeled with '*' represents DSF (100 μg/mL) + Chumacin-1 (MIC-3.9 μg/mL-9.39 μM) and the well labeled with '#' represent DSF (100 μg/mL) + Chumacin-2 (MIC-3.9 μg/mL-9.42 μM). The control wells were loaded with DSF alone (100 μg/mL).

signal. The bacterial reponse to each quorum signal may vary (Bassler and Losick, 2006; Williams, 2007; Diggle et al., 2007). In the present study, the effect of Chumacin-1 and Chumacin-2 was evaluated on quorum sensing signaling mechanism of a quorum sensing reporter strain, *Chromobacterium violaceum* strain CV026 using the commercial quorum sensing signal factor, DSF derived from *X. campestris*. Interestingly, the assay revealed that the strain CV026 responded to the DSF *in vitro*. This could be the result of interspecies quorum sensing cross talk between strain CV026 and DSF. This assay also revealed that both Chumacin-1 and Chumacin-2 at their corresponding MICs inhibited the quorum sensing mechanism as evident from the lack of violacein production. At lower concentrations than their MIC, Chumacin-1 and Chumacin-2 could not inhibit violacein production. The results suggested that both Chumacin-1 and Chumacin-2 extrolites efficiently inhibited the quorum sensing signaling mechanism at their MIC of 3.9 μg/mL, even in the presence of externally supplemented DSF. The control group treated with DSF supplementation showed violacein pigmentation (Fig. 2).

3.4. Diffusible signal factor (DSF) extraction, detection and quantification

The excellent performance of Chumacin-1 and Chumacin-2 as potential inhibitors of growth, biofilm formation, xanthan gum and quorum sensing in various *Xanthomonas* pathovars, has led us to further explore their effect on the key quorum sensing signal, *cis*-11-methyl-dodecenoic acid. The Gram-negative bacteria, including *Xanthomonas* communicate with each other using the widely conserved signaling molecules belonging to the diffusible signal factor (DSF) family (Deng et al., 2011). The detection and quantification of *cis*-11-methyl-dodecenoic acid is very significant to understand the ability of the candidate antimicrobials as an effective strategy to combat the resistance acquisition by pathogens. One study suggested that DSF in *Xanthomonas campestris* could possibly act as a kick start signal for the biofilm-aggregate-planktonic transition. The biofilm formation and dispersal in *Xanthomonas campestris* is under the control of DSF signaling indicating the intriguing complexity and tight control of the quorum sensing at molecular level (Dow et al., 2003). Antimicrobials that could inhibit quorum sensing signaling are the need of the hour as they can overcome the problems encountered from the conventional chemicals that result in selective pressure on pathogens, just by killing or inhibiting the pathogen growth. The quorum sensing inhibitors work as smart antimicrobials (one bullet for multiple targets) that confuse and weaken the pathogens by targeting multiple virulence factors like biofilm, EPS and growth inhibition, that are under the control of quorum sensing, at a time. In *X. oryzae* pv. *oryzae*, a bacterial pathogen causing bacterial blight of rice, quorum sensing network uses a DSF, i.e. *cis*-11-methyl-dodecenoic acid to regulate pathogenicity. The DSF expression is controlled by *rpf* (regulation of pathogenicity factor) gene members and the enzymes coded by *rpf* gene family. This implies that breaking this DSF expression could control the infection caused by *X. oryzae* pv. *oryzae*. In this context, the effect of Chumacin-1 and Chumacin-2 were studied on the DSF secretion by *X. oryzae* pv. *oryzae* strain TNAU-2. Strain TNAU-2 treated with Chumacin-1, Chumacin-2 and the corresponding control groups were subjected to DSF extraction followed by HPLC detection. The HPLC chromatograms revealed the presence of DSF peaks in the untreated (control) groups of *X. oryzae* pv. *oryzae* strain TNAU-2 at the retention times of 3.552 min and 5.585 min (Supplementary Fig. S13a), whereas the chromatograms of Chumacin-1 and Chumacin-2 did not show any peaks corresponding to the DSF (Supplementary Figs. S13b and S13c), indicating the absence of extracellular DSF, which was also confirmed by HRMS spectra (Supplementary Figs. S14a, 14b and 14c), that showed absence of the characteristic peaks corresponding to DSF. In the present study, the effect of Chumacin-1 [3.9 μg/mL (9.39 μM)] and Chumacin-2 [3.9 μg/mL (9.42 μM)] extrolites on the DSF produced

by strain TNAU-2 was also analyzed by mass spectrometry. Interestingly, both Chumacin-1 and Chumacin-2 treated groups of strain TNAU-2, did not show characteristic peaks of DSF (m/z value of 213.1250) in the mass spectrum ($M+H^+$), indicating that Chumacin-1 and Chumacin-2 negatively effected the DSF production by strain TNAU-2. While in the untreated control group, the DSF peak at m/z value of 213.1250 was observed. Hence, it is clear that the *P. aeruginosa* strain CGK-KS-1 derived Chumacin-1 and Chumacin-2 inhibited the key quorum sensing signal, DSF in *X. oryzae* pv. *oryzae* strain TNAU-2.

3.5. Xanthan gum inhibition

The promising results shown by Chumacin-1 and Chumacin-2 in the antimicrobial assay, and quorum sensing overlay assay have inspired us to further explore their effect on the key virulence factor of *Xanthomonads,* the EPS or xanthan gum. Xanthan gum is a vital virulent component for the Xanthomonads to form biofilms, maintain their stability and protect the biofilm in-dwelling cells from harmful external factors. In the present study, the effect of Chumacin-1 and Chumacin-2 extrolites was studied on the amount of xanthan gum produced by *X. campestris* pv. *campestris* MTCC 2286 (prolific producer of xanthan gum). Both the bioactive extrolites showed a decrease in the xanthan gum yield. Chumacin-1 reduced the xanthan gum content by 67%, while Chumacin-2 reduced the xanthan gum content by 56% and copper oxychloride showed reduction by just 17% (Fig. 3 and Supplementary Fig. S15). Similar observations were reported in previous studies with other Xanthomonads, where chemical agents like sulfone derivatives (Shi et al., 2015), azole derivatives (Liang et al., 2016), thymol (Singh et al., 2017) and niclosamide (Sahu et al., 2018) showed reduced xanthan gum production. The results suggested that both Chumacin-1 and Chumacin-2 were able to suppress the virulence factor of *X. campestris* pv. *campestris* MTCC 2286.

3.6. Anti-biofilm activity

Xanthomonads form self-organized groups or biofilms as an alternative living mode to escape external stress factors like other dominating microbes, temperature, pH, salinity, antibiotics, agrochemicals or drugs. A specialized matrix composed of an extracellular polysaccharide or xanthan gum secreted by *Xanthomonas* bacterial cells, forms the structural basis of the biofilm. Moreover the transitions between planktonic state, biofilm state, aggregation or dispersion of biofilms helps the bacteria to invade a plant host and exert pathogenicity. Hence, there is a need for efficient control methods that can disrupt biofilms formed by pathogenic bacteria. Some of the natural biofilm and/or quorum sensing inhibitors reported in the recent past

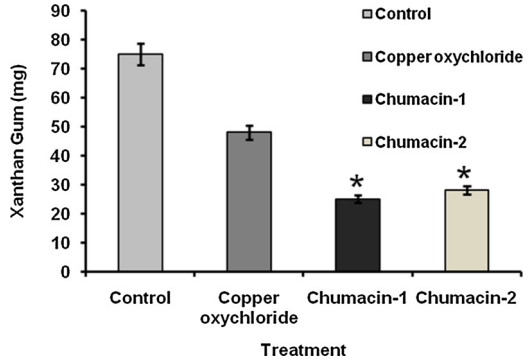

Fig. 3. Quantification of xanthan gum produced by *Xanthomonas campestris* pv. *campestris* MTCC 2286 treated with Chumacin-1 and Chumacin-2. *X. campestris* pv. *campestris* MTCC 2286 was treated with Chumacin-1 and Chumacin-2, while the untreated and Copper oxychloride treated groups were also quantified in parallel as controls.

including halogenated furanone from red alga *Delisea pulchra* (Gram et al., 1996), 4-phenylbutanoic acid produced by marine bacterium *Bacillus pumilus* S6-15 (Nithya et al., 2011), PAM galactan produced by *Kingella kingae* (Bendaoud et al., 2011), cinnamic acid and proline-derived linear dipeptides proline–glycine and N-amido-α-proline derived from marine *Streptomyces* sp. NIO 10,068 (Naik et al., 2013), piericidin A1, 3′-rhamnopiericidin A1 and piericidin E derived from *Streptomyces* sp. TOHO-Y(Ooka et al., 2013) along with piericidin A and glucopiericidin A produced by *Streptomyces xanthocidicus* KPP01532 (Kang et al., 2016), which are significant from the perspective of their biodegradability and innate antagonism towards plant pathogens. There are very few reports on the inhibitors of *Xanthomonas* biofilms, including thyme oil reducing biofilm formation in *X. oryzae* (Singh et al., 2017), niclosamide blocking biofilm formation in *X. oryzae* (Sahu et al., 2018), monoacylglycerols blocking biofilms in *X. oryzae* (Ham and Kim, 2016), imidazole derivatives inhibiting biofilms in *Xanthomonas* sp. (Melander et al., 2015). Since *Xanthomonas* biofilm formation is one of the important virulence factor, the effect of Chumacin-1 and Chumacin-2 was studied on the biofilms formed by a panel of *Xanthomonas* pathogens and the results to this regard are presented in the Table 2. Interestingly, both the bioactives, Chumacin-1 and Chumacin-2, inhibited the biofilms formed by all the test panel pathogens at IC_{50} value below 45 μM. While copper oxychloride inhibited the *Xanthomonas* biofilms with an IC_{50} value of more than 350 μM. In a recent report, the small molecule anthranilamide produced by *Streptomyces* spp. inhibited the biofilm formed by *Xanthomonas oryzae* at a very higher concentration of ˜50 μg/mL (1100 μM) (Ham and Kim, 2018), which was almost 100-fold higher as compared to that of biofilm inhibition by Chumacin-1 [3.9 μg/mL (9.39 μM)] and Chumacin-2 [3.9 μg/mL (9.42 μM)]. Further, the biofilm inhibition exhibited towards *X. oryzae* pv. *oryzae* strain TNAU-2 by Chumacin-1 and Chumacin-2 was visualized by FE-SEM and the results to this regard are shown in Fig. 4A. It was observed that the untreated cells of *X. oryzae* pv. *oryzae* showed an intact biofim formation with thick EPS and tightly packed cells inside the biofilm matrix (Fig. 4A, panel-a). While the *X. oryzae* pv. *oryzae* cells treated with Chumacin-1 and Chumacin-2 showed a disrupted biofilm and EPS with cell lysis and membrane disruption of indwelling cells (Figs. 4A, panel-b and panel-c). These results are similar to the results of other studies. Further, SEM observations revealed that niclosamide inhibited the biofilm formation in *Xanthomonas oryzae* at a higher concentration of 5 μg/mL (15.28 μM) (Sahu et al., 2018), as compared to that of biofilm inhibition by Chumacin-1 [3.9 μg/mL (9.39 μM)] and Chumacin-2 [3.9 μg/mL (9.42 μM)]. The observations from the current study reveals that Chumacin-1 and Chumacin-2 could effectively disrupt the biofilm formed by *X. oryzae* pv. *oryzae* strain TNAU-2 at very low concentrations.

3.7. Confocal scanning laser microscopy

Most of the antimicrobials exert antibiotic effect by altering or disrupting the cell membrane. The cell membrane plays an important role in the maintanance of structure, integrity and survival of any living cell. The effect of Chumacin-1 and Chumacin-2 on *X. oryzae* pv. *oryzae* strain TNAU-2 membrane at their corresponding minimum inhibitory concentrations was also visualized by CSLM and the micrographs to this regard are shown in Fig. 4B. Based on the confocal micrographs, it was observed that strain TNAU-2 cells of untreated control group (Fig. 4B, panel-a) were alive with an intact cell membrane as indicated by green fluorescence emitted by SYTO9, while the cells treated with Chumacin-1 and Chumacin-2 were dead (Fig. 4B, panel-b and panel-c) with a damaged cell membrane as indicated by DNA staining with propidium iodide that entered the cytoplasm because of the membrane damage, since propidium iodide enters only the damaged membranes and imparts red fluorescence to the treated cells. These results suggest that Chumacin-1 and Chumacin-2 extrolites exhibited a cell membrane damaging effect on *X. oryzae* pv. *oryzae*. The staining of live and dead cells of *X. oryzae* pv. *oryzae* in the current study is similar to that observed in

Table 2
Biofilm inhibitory activity of Chumacin-1 and Chumacin-2 against different species and strains of *Xanthomonas* pathovars.

Test pathogens	MBIC (μM)			
	Chumacin-1	Chumacin-2	Copper oxychloride	Tetracycline
Xanthomonas oryzae pv. *oryzae* strain TNAU-2	23.19 ± 0.06	27.13 ± 0.21	596.12 ± 0.17	–
X. oryzae pv. *oryzicola* strain Y2	32.11 ± 0.12	28.12 ± 0.31	550.01 ± 0.26	–
X. campestris pv. *vesicatoria* strain XIS	28.17 ± 0.07	26.21 ± 0.20	592.04 ± 0.23	–
X. campestris pv. *vesicatoria* strain 65-10	23.00 ± 0.08	28.26 ± 0.22	650.10 ± 0.23	–
X. campestris pv. *vesicatoria* strain 85-10	40.7 ± 0.04	27.26 ± 0.11	656.04 ± 0.32	–
X. campestris pv. *vesicatoria* strain 8004	25.00 ± 0.04	30.00 ± 0.18	570.02 ± 0.06	–
X. campestris pv. *campestris* strain C1	22.16 ± 0.04	29.13 ± 0.09	580.15 ± 0.18	–
X. campestris pv. *campestris* strain TNAU-1	28.23 ± 0.14	31.06 ± 0.03	750.06 ± 0.27	–
X. campestris pv. *campestris* MTCC 2286	31.33 ± 0.11	33.02 ± 0.10	759.23 ± 0.20	–
Chromobacterium violaceum strain CV026	20.11 ± 0.03	21.16 ± 0.05	–	19.36 ± 0.04

MBIC: Minimum Biofilm Inhibitory Concentration is the least concentration of an antimicrobial agent that causes no observable test microbial growth in the wells, as adherent biofilm or microcolonies. (MBIC is expressed in μM at $P < 0.05$).

the case of fluorescence micrographs of live and dead cells of *Xanthomonas axonopodis* pv. *phaseoli* in which the propidium iodide stained only the damaged cell membranes (Tebaldi et al., 2010). Further, these results are in correlation with the FE-SEM observations of the current study, that showed damaged cell membranes in *X. oryzae* pv. *oryzae* biofilms treated with Chumacin-1 and Chumacin-2 (Section 3.6 - Antibiofilm activity). The FE-SEM micrographs also showed altered morphology of the cells and detrimental effect of Chumacin-1 and Chumacin-2 to the membrane integrity, that could have possibly resulted in the lysis of the cell membrane or pore formation, leading to the death of strain TNAU-2 cells. The intracellular ROS generated by Chumacin-1 and Chumacin-2 might be the cause for damage of cell membrane in *X. oryzae* pv. *oryzae*.

3.8. ROS quantification

Reactive oxygen species cause damage to nucleic acids, proteins, membrane lipids and organelles owing to the presence of highly reactive electrons. The effect of Chumacin-1 and Chumacin-2 on various *Xanthomonas* strains was observed by NBT-based ROS assay, which enables spectrophotometric measurement of generated superoxide ions. The $OD_{540\ nm}$, the measure of ROS generated, was approximately three

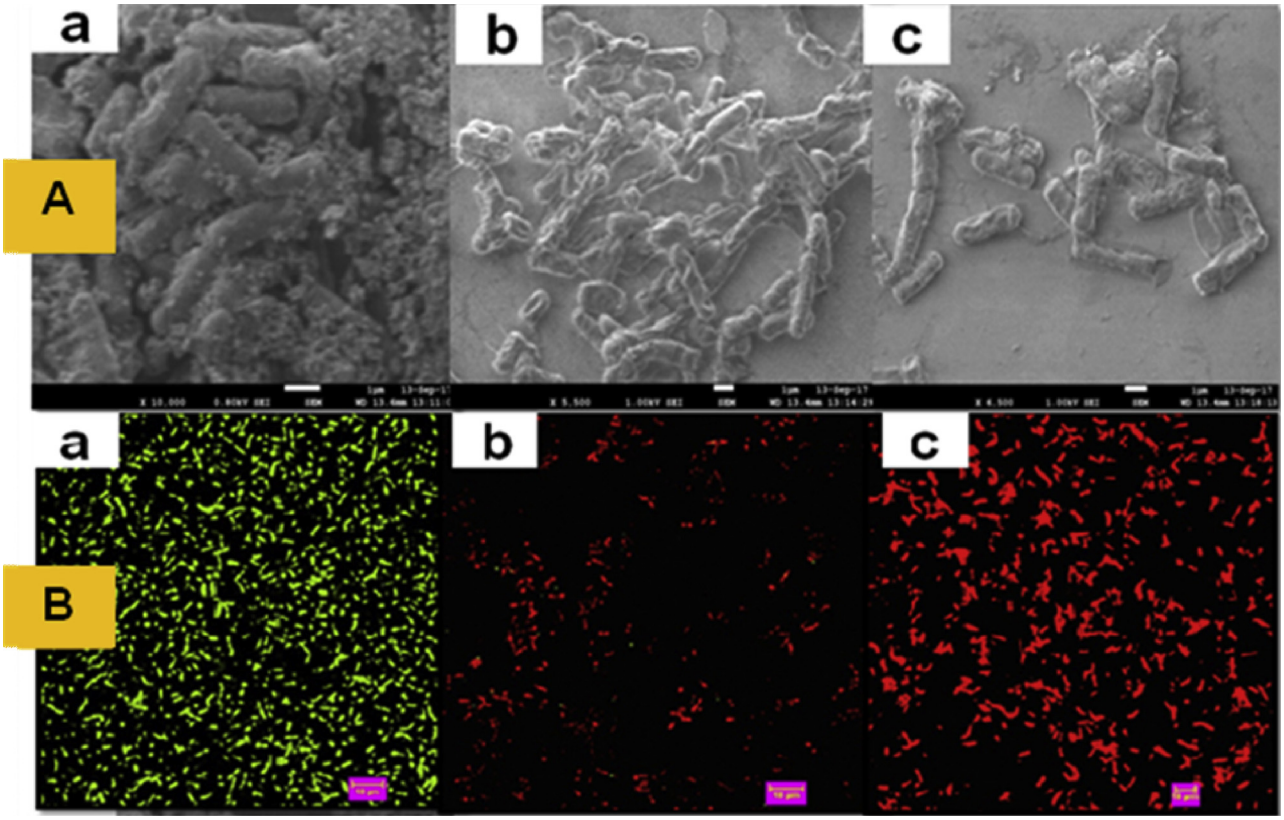

Fig. 4. (A) FE-SEM micrographs of biofilms formed by *Xanthomonas oryzae* pv. *oryzae* strain TNAU-2 treated with Chumacin-1 and Chumacin-2. (a) Control group of *X. oryzae* pv. *oryzae* strain TNAU-2, with intact biofilm matrix and cell morphology, (b) Chumacin-1 (MIC value 3.9 μg/mL, 9.39 μM) treated *X. oryzae* pv. *oryzae* strain TNAU-2 cells with disrupted biofilm and damaged cell membrane, and (c) Chumacin-2 (MIC value 3.9 μg/mL, 9.42 μM) treated *X. oryzae* pv. *oryzae* strain TNAU-2 cells with disrupted biofilm and damaged cell membrane. (B) CSLM micrographs of *X. oryzae* pv. *oryzae* strain TNAU-2 cells treated with Chumacin-1 and Chumacin-2. (a) Untreated (control) group of *X. oryzae* pv. *oryzae* strain TNAU-2, with intact cell membrane, as stained by live cell specific stain, SYTO-9. (b) Chumacin-1 (MIC value 3.9 μg/mL, 9.39 μM) and (c) Chumacin-2 (MIC value 3.9 μg/mL, 9.42 μM) treated *X. oryzae* pv. *oryzae* strain TNAU-2 cells showing damaged cell membrane as revealed by cellular DNA stained with propidium iodide, that enters cells through damaged membranes.

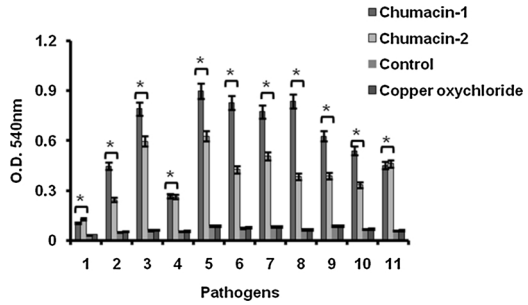

Fig. 5. ROS quantification in different species and strains of *Xanthomonas* pathovars treated with Chumacin-1 and Chumacin-2. All the *Xanthomonas* species and strains, (1) *Xanthomonas oryzae* strain TNAU-2, (2) *X. oryzae* pv. *oryzicola* strain Y2, (3) *X. campestris* pv. *vesicatoria* strain XIS, (4) *X. campestris* pv. *vesicatoria* strain 65-10, (5) *X. campestris* pv. *vesicatoria* strain 85-10, (6) *X. campestris* pv. *vesicatoria* strain 8004, (7) *X. campestris* pv. *campestris* strain C1, (8) *X. campestris* pv. *campestris* strain TNAU-1, (9) *X. campestris* pv. *campestris* MTCC 2286, and (10) *X. axonopodis.* pv. *punicae* strain XAP-97 were treated with Chumacin-1 (MIC value 3.9 µg/mL, 9.39 µM) and Chumacin-2 (MIC value 3.9 µg/mL, 9.42 µM) which induced ROS generation. $O.D._{540\ nm}$ corresponds to amount of ROS generated. The '*' indicates the statistical significance of ROS generated between the Chumacin-1 and Chumacin-2 treated groups and Copper oxychloride and control groups of various pathogens ($P < 0.05$).

to four folds higher than the control group in all the different *Xanthomonas* strains treated with Chumacin-1 and Chumacin-2. The absorbance at 540 nm was directly proportional to the amount of intracellular ROS generated by Chumacin-1 and Chumacin-2 (Fig. 5). These results suggest that Chumacin-1 and Chumacin-2 generated two to three folds higher intracellular ROS in all the test *Xanthomonas* and *Chromobacterium* strains, whereas the OD_{540} was very negligible in the cells treated with the Copper oxychloride and untreated control cells. Wherein, the ROS generated by the Chumacin-1 and Chumacin-2 was much lower in the *X. oryzae.* pv. *oryzae* strain BXO43 and *C. violaceum* strain CV026 as compared to the corresponding ROS generated in other pathogens. Further, these results also suggest that Chumacin-1 and

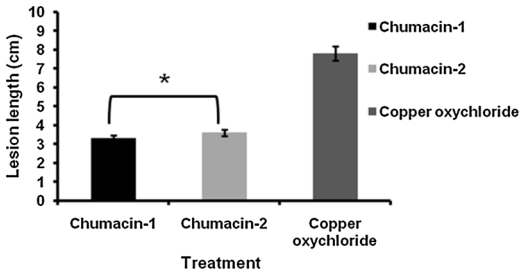

Fig. 7. Leaf migration assay after 3 weeks of infection, to evaluate the migration distance of *Xanthomonas oryzae* pv. *oryzae* strain TNAU-2 in rice plants after treatment with Chumacin-1 and Chumacin-2. The '*' indicates statistically significant difference in the leaf migration distance of strain TNAU-2 between the Chumacin-1 and Chuamcin-2 treated group of plants and Copper oxychloride treated group of plants ($P < 0.05$).

Chumacin-2 generate ROS that may damage the cell membrane, as visualized in the CSLM and FE-SEM micrographs in the current study (Section- Confocal scanning laser microscopy and Antibiofilm activity). These results also suggest that Chumacin-1 and Chumacin-2 may exert multiple modes of action to inhibit the Xanthomonads.

3.9. Greenhouse studies

The promising observations of Chumacin-1 and Chumacin-2 effecting the inhibition of growth, biofilm formation, xanthan gum secretion and quorum sensing has led us to further validate these observations under greenhouse conditions by exploring their effect on control of bacterial blight of rice. The greenhouse experiments showed that Chumacin-1 and Chumacin-2 extrolites efficiently inhibited bacterial blight caused by *X. oryzae* pv. *oryzae* strain TNAU-2 in rice plants. The effect of seed treatment and foliar spray with Chumacin-1 and Chumacin-2 extrolites was studied on the rice plants in comparison with copper oxychloride as standard for seed treatment. The treated seeds were used for further germination and plant growth. After three

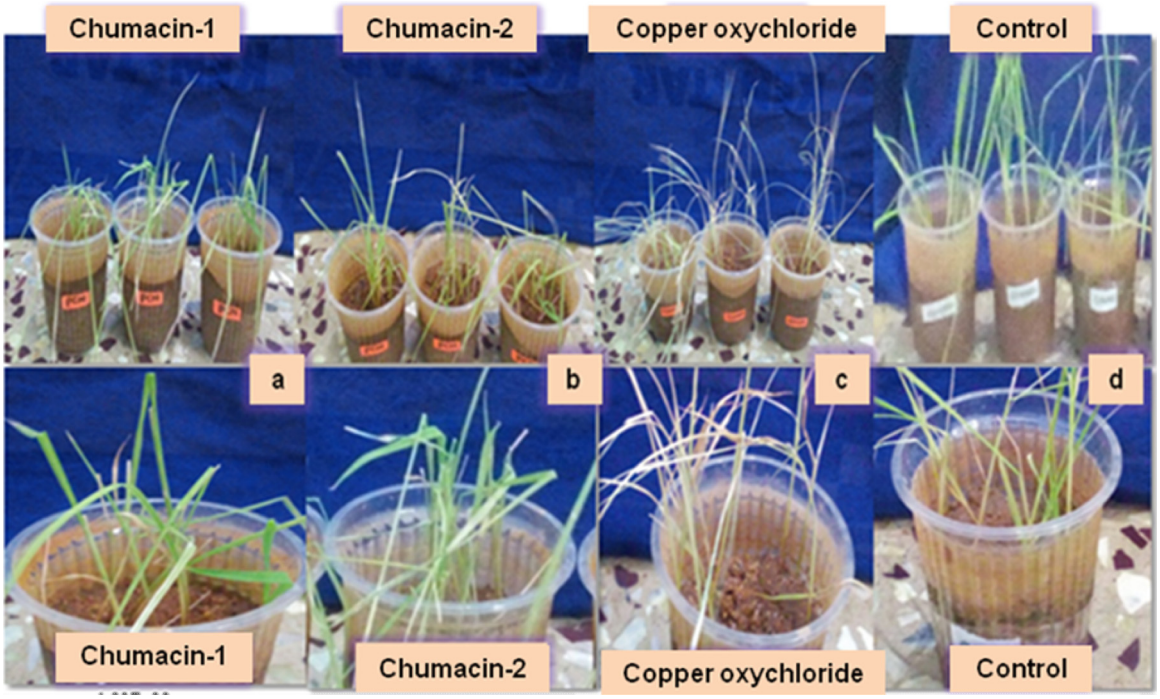

Fig. 6. Greenhouse experiments showing rice plants treated with Chumacin-1 and Chumacin-2 to understand their functional role in the control of bacterial blight of rice. The rice plants were infected with *Xanthomonas oryzae* pv. *oryzae* strain TNAU-2 followed by treatment with (a) Chumacin-1, (b) Chumacin-2 and (c) Copper oxychloride. (d) Uninfected rice plants which served as negative control.

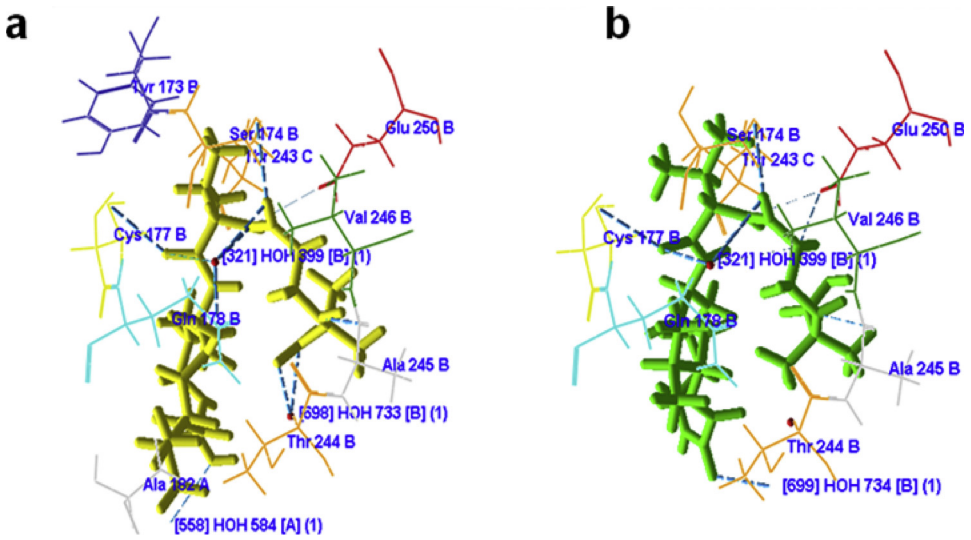

Fig. 8. Molecular docking of Chumacin-1 and Chumacin-2 with *RpfF* pocket of *Xanthomonas campestris* pv. *campestris*. Interaction of (a) Chumacin-1 and (b) Chumacin-2 with the residues of *RpfF* pocket.

weeks of germination, the plants were infected with *X. oryzae* pv. *oryzae* strain TNAU-2 and the disease progress was monitored for three weeks. It was observed that after three weeks of infection, the plants generated from seed treated with bioactive extrolites and also with foliar spray were healthy and normal with good leaf length and leaf weight as compared to the Copper oxychloride treated counterparts (Figs. 6a-6d). The virulence assay revealed that in the plants treated with Chumacin-1 and Chumacin-2, the pathogen migrated upto less than 3.3 ± 0.03 cm and 3.6 ± 0.12 cm on an average from the point of infection, whereas in the Copper oxychloride treated plants, the pathogen migrated an average distance of 7.9 ± 0.06 cm, after 3 weeks of infection (Fig. 7). These greenhouse experimental results suggest that *P. aeruginosa* strain CGK-KS-1 derived extrolites efficiently suppressed the bacterial blight of rice caused by *X. oryzae* pv. *oryzae* strain TNAU-2.

3.10. Molecular docking

The impressive property of Chumacin-1 and Chumacin-2 as inhibitors of cis-11-methyl-dodecenoic acid (DSF), has led us to observe their effect on the *rpfF* enzyme that synthesizes DSF, *in silico*. The *Xanthomonas* quorum sensing signals or diffusible signal factor expression, perception, response and degradation are under the control of gene family of *rpf* (regulation of pathogenicity factors). The *rpf* family comprises of *rpfA-rpfG* genes. The *rpfF* gene codes for DSF synthase, an enzyme that synthesizes a key quorum sensing signal, *cis*-11-methyl-dodecenoic acid in various *Xanthomonas* pathovars (Chatterjee and Sonti, 2002). The bioactive molecules that bind and inhibit *rpfF* target make an attractive choice for effectively combating the signal transduction mechanism which mediates the quorum sensing phenomenon in plant pathogens. Chumacin-1 (Fig. 8a) and Chumacin-2 (Fig. 8b) docked well with the pocket of *rpfF* with docking scores of -91.867 and -101.532. The detailed binding energies of the Chumacin-1 and Chumacin-2, their interactions with the *rpfF* pocket are given in the Supplementary Table S4. These results suggest that both these extrolites may bind strongly to the *rpfF* which inhibits DSF synthesis and blocks quorum sensing signalling. These *in silico* docking studies were in correlation with the observations made in DSF quantification by HRMS that showed absence of DSF peaks in the Chumacin-1 and Chumacin-2 treated *X. oryzae* pv. *oryzae* of the current study (Section-.Diffusible signal factor (DSF) extraction, detection and quantification).

4. Conclusions

Overall, the results suggest that Chumacin-1 and Chumacin-2 may possibly alter the quorum sensing signaling system in *X. oryzae* pv. *oryzae* strain TNAU-2 that led to the DSF inhibition, xanthan gum reduction, biofilm disruption, cell membrane disruption and reduced virulence. Chumacin-1 and Chumacin-2 also showed ROS generation in the tested *Xanthomonas* strains that might have possibly led to their cell membrane disruption. Further this study showed that Chumacin-1 and Chumacin-2 effectively controlled bacterial blight in the rice plants. Moreover, the extrolites Chumacin-1 and Chumacin-2 showed promising inhibition of various other *Xanthomonas* pathogens *in vitro*. *In silico* docking studies showed that Chumacin-1 and Chumacin-2 binds and inhibits the DSF synthase, which is in correlation with the HRMS results. Moreover, it was observed that DSF could induce quorum sensing cross talk in *Chromobacterium violaceum* strain CV026. Chumacin-1 and Chumacin-2 could also inhibit this quorum cross talk between *X. campestris* and *C. violaceum* strain CV026. Thus this study offers an intriguing strategy which could be applied as a better alternative for the control of *X. oryzae* pv.*oryzae* and other Xanthomonads. However, further field studies, toxicological analyses and molecular studies are necessary for understanding the exact mechanism of action and application of these bacterial extrolites as effective biocontrol agents.

Declarations of interest

None.

Acknowledgements

The authors acknowledge the financial assistance provided to Ms. K. Sirisha in the form of Junior Research Fellowshipby Department of Biotechnology, Government of India, New Delhi. The authors are thankful to Prof. Appa Rao Podile, Vice Chancellor, University of Hyderabad, Hyderabad, for extending the greenhouse facility to carry out the relevant experiments. The authors are also thankful to Dr. S. Kartikeyan, Microbiology Department, Tamil Nadu Agricultural University, Coimbatore for sharing some of the *Xanthomonas* cultures for our research work. IICT Manuscript Communication No. IICT/Pubs./2019/212.

Appendix A. Supplementary data

Supplementary material related to this article can be found, in the online version, at doi:https://doi.org/10.1016/j.micres.2019.126301.

References

Amsterdam, D., 1996. Susceptibility testing of antimicrobials in liquid media. In: Loman, V. (Ed.), Antibiotics in Laboratory Medicine., 4th ed. Williams and Wilkins, Baltimore, MD, pp. 61–143.

Bano, N., Musarrat, J., 2003. Characterization of a new *Pseudomonas aeruginosa* strain NJ-15 as a potential biocontrol agent. Curr. Microbiol. 46, 324–328. https://doi.org/10.1007/s00284-002-3857-8.

Bassler, B.L., Losick, R., 2006. Bacterially speaking. Cell 125, 237–246. https://doi.org/10.1016/j.cell.2006.04.001.

Bendaoud, M., Vinogradov, E., Balashova, N.V., Kadouri, D.E., Kachlany, S.C., Kaplan, J.B., 2011. Broad-spectrum biofilm inhibition by *Kingella kingae* exopolysaccharide. J. Bacteriol. 193, 3879–3886. https://doi.org/10.1128/jb.00311-11.

Bernal, P., Allsopp, L.P., Filloux, A., Llamas, M.A., 2017. The *Pseudomonas putida* T6SS is a plant warden against phytopathogens. ISME J. 11, 972–987. https://doi.org/10.1038/ismej.2016.169.

Chatterjee, S., Sonti, R.V., 2002. *rpfF* mutants of *Xanthomonas oryzae* pv. *oryzae* are deficient in virulence and growth under low iron conditions. Mol. Plant Microbe Interact. 15, 463–471. https://doi.org/10.1094/MPMI.2002.15.5.463.

Chin-A-Woeng, T.F., Bloemberg, G.V., Lugtenberg, B.J., 2003. Phenazines and their role in biocontrol by *Pseudomonas* bacteria. New Phytol. 157, 503–523. https://doi.org/10.1046/j.1469-8137.2003.00686.x.

Chin-A-Woeng, T.F., Bloemberg, G.V., Mulders, I.H., Dekkers, L.C., Lugtenberg, B.J., 2000. Root colonization by phenazine-1-carboxamide-producing bacterium *Pseudomonas chlororaphis* PCL1391 is essential for biocontrol of tomato foot and root rot. Mol. Plant Microbe Interact. 13, 1340–1345. https://doi.org/10.1094/mpmi.2000.13.12.1340.

Choma, I.M., Grzelak, E.M., 2011. Bioautography detection in thin-layer chromatography. J. Chromatogr. A 1218, 2684–2691. https://doi.org/10.1016/j.chroma.2010.12.069.

Christensen, G.D., Simpson, W.A., Younger, J.J., Baddour, L.M., Barrett, F.F., Melton, D.M., Beachey, E.H., 1985. Adherence of coagulase negative staphylococci to plastic tissue culture plates: a quantitative model for the adherence of staphylococci to medical devices. J. Clin. Microbiol. 22, 996–1006. https://doi.org/10.1007/BF02017694.

Debode, J., Maeyer, K.D., Perneel, M., Pannecoucque, J., Backer, G.D., Höfte, M., 2007. Biosurfactants are involved in the biological control of *Verticillium* microsclerotia by *Pseudomonas* spp. J. Appl. Microbiol. 103, 1184–1196. https://doi.org/10.1111/j.1365-2672.2007.03348.x.

Deng, Y., Wu, J., Tao, F., Zhang, L.H., 2011. Listening to a new language: DSF-based quorum sensing in Gram-negative bacteria. Chem. Rev. 111, 160–173. https://doi.org/10.1021/cr100354f.

Dharmapuri, S., Sonti, R.V., 1999. A transposon insertion in the gumG homologue of *Xanthomonas oryzae* pv. *oryzae* causes loss of extracellular polysaccharide production and virulence. FEMS Microbiol. Lett. 179, 53–59. https://doi.org/10.1016/s0378-1097(99)00367-5.

Diggle, S.P., Griffin, A.S., Campbell, G.S., West, S.A., 2007. Cooperation and conflict in quorum-sensing bacterial populations. Nature 450, 411–414. https://doi.org/10.1038/nature06279.

Dong, Y.H., Wang, L.H., Xu, J.L., Zhang, H.B., Zhang, X.F., Zhang, L.H., 2001. Quenching quorum-sensing-dependent bacterial infection by an *N*-acyl homoserine lactonase. Nature 411, 813–817. https://doi.org/10.1038/35081101.

Dow, J.M., Crossman, L., Findlay, K., He, Y., Feng, J., Tang, J., 2003. Biofilm dispersal in *Xanthomonas campestris* is controlled by cell-cell signaling and is required for full virulence to plants. Proc. Natl. Acad. Sci. U.S.A. 100, 10995–11000. https://doi.org/10.1073/pnas.1833360100.

Expert, J.M., Digat, B., 1995. Biocontrol of *Sclerotinia* wilt of sunflower by *Pseudomonas fluorescens* and *Pseudomonas putida* strains. Can. J. Microbiol. 41, 685–691. https://doi.org/10.1139/m95-094.

Ferluga, S., Steindler, L., Venturi, V., 2008. *N*-acyl homoserine lactone quorum sensing in Gram-negative rhizobacteria. In: Karlovsky, P. (Ed.), Secondary Metabolites in Soil Ecology. Springer, Berlin, Germany, pp. 69–90. https://doi.org/10.1007/978-3-540-74543-3_4.

Flahive, J.J., Foufopoulos, A., Etzel, M.R., 1994. Alcohol precipitation of xanthan gum from pure solutions and fermentation broths. Sep. Sci. Technol. 29, 1673–1687. https://doi.org/10.1080/01496399408002164.

Flemming, H., Wingender, J., 2010. The biofilm matrix. Nat. Rev. Microbiol. 8, 623–633. https://doi.org/10.1038/nrmicro2415.

Gram, L., de Nys, R., Maximilien, R., Givskov, M., Steinberg, P., Kjelleberg, S., 1996. Inhibitory effects of secondary metabolites from the red alga *Delisea pulchra* on swarming motility of *Proteus mirabilis*. Appl. Environ. Microbiol. 62, 4824–4827.

Ham, Y., Kim, T., 2018. Anthranilamide from *Streptomyces* spp. inhibited *Xanthomonas oryzae* biofilm formation without affecting cell growth. Appl. Biol. Chem. 61, 673–680. https://doi.org/10.1007/s13765-018-0405-1.

Ham, Y., Kim, T.J., 2016. Inhibitory activity of monoacylglycerols on biofilm formation in *Aeromonas hydrophila*, *Streptococcus mutans*, *Xanthomonas oryzae*, and *Yersinia enterocolitica*. SpringerPlus 2016 5, 1526. https://doi.org/10.1186/s40064-016-3182-5.

Hancock, R., 1997. The bacterial outer membrane as a drug barrier. Trends Microbiol. 5, 37–42. https://doi.org/10.1016/s0966-842x(97)81773-8.

He, Y., Zhang, L., 2008. Quorum sensing and virulence regulation in *Xanthomonas campestris*. FEMS Microbiol. Rev. 32, 842–857. https://doi.org/10.1111/j.1574-6976.2008.00120.x.

Hedin, P.A., 1982. New concepts and trends in pesticide chemistry. J. Agric. Food Chem. 30, 201–215. https://doi.org/10.1021/jf00110a001.

Kang, J.E., Han, J.W., Jeon, B.J., Kim, B.S., 2016. Efficacies of quorum sensing inhibitors, piericidin A and glucopiericidin A, produced by *Streptomyces xanthocidicus* KPP01532 for the control of potato soft rot caused by *Erwinia carotovora* subsp. *atroseptica*. Microbiol. Res. 184, 32–41. https://doi.org/10.1016/j.micres.2015.12.005.

Kim, S., Song, J.T., Jeong, J., Seo, H.S., 2016. Niclosamide inhibits leaf blight caused by *Xanthomonas oryzae* in rice. Sci. Rep. 6, 21209. https://doi.org/10.1038/srep21209.

Kulshreshtha, G., Velusamy, G., 2012. Antibacterial potential of bioactive compounds from fermented culture of *Pseudomonas aeruginosa* SRM1 against *Xanthomonas oryzae* pv. *oryzae*. Minerva Biotecnol. 24, 29–36.

Lanteigne, C., Gadkar, V.J., Wallon, T., Novinscak, A., Filion, M., 2012. Production of DAPG and HCN by *Pseudomonas* sp. LBUM300 contributes to the biological control of bacterial canker of tomato. Phytopathology 102, 967–973. https://doi.org/10.1094/phyto-11-11-0312.

Liang, X., Yu, X., Pan, X., Wu, J., Duan, Y., Wang, J., Zhou, M., 2016. A thiadiazole reduces the virulence of *Xanthomonas oryzae* pv. *oryzae* by inhibiting the histidine utilization pathway and quorum sensing. Mol. Plant Pathol. 19, 116–128. https://doi.org/10.1111/mpp.12503.

Mazurier, S., Corberand, T., Lemanceau, P., Raaijmakers, J.M., 2009. Phenazine antibiotics produced by fluorescent pseudomonads contribute to natural soil suppressiveness to *Fusarium* wilt. ISME J. 3, 977–991. https://doi.org/10.1038/ismej.2009.33.

Melander, C., Cavanagh, J., Ritchie, D., Huigens III R.W., Ballard, T.E., Richards, J.J., Lindsey, T.W., Lindsey, J.S., 2015. Inhibition of biofilms in plants with imidazole derivatives. US 8927029B2 (Assigned to North Carolina State University, Raleigh, NC, USA).

Michelsen, C.F., Watrous, J., Glaring, M.A., Kersten, R., Koyama, N., Dorrestein, P.C., Stougaard, P., 2015. Nonribosomal peptides, key biocontrol components for *Pseudomonas fluorescens* In5, isolated from a Greenlandic suppressive soil. mBio 6, 1–9. https://doi.org/10.1128/mbio.00079-15.

Munhoz, L.D., Fonteque, J.P., Santos, I.M., Navarro, M.O., Simionato, Goya, E.T., Rezende, M.I., Balbi-Peña, M.I., de Oliveira, A.G., Andrade, G., 2017. Control of bacterial stem rot on tomato by extracellular bioactive compounds produced by *Pseudomonas aeruginosa* LV strain. Cogent Food Agric. 3, 1–16. https://doi.org/10.1080/23311932.2017.1282592.

Naik, D., Wahidullah, S., Meena, R., 2013. Attenuation of *Pseudomonas aeruginosa* virulence by marine invertebrate-derived *Streptomyces* sp. Lett. Appl. Microbiol. 56, 197–207. https://doi.org/10.1111/lam.12034.

Nithya, C., Devi, M.G., Karutha Pandian, S., 2011. A novel compound from the marine bacterium *Bacillus pumilus* S6-15 inhibits biofilm formation in Gram-positive and Gram-negative species. Biofouling 27, 519–528. https://doi.org/10.1080/08927014.2011.586127.

Ooka, K., Fukumoto, A., Yamanaka, T., Shimada, K., Ishihara, R., Anzai, Y., Kato, F., 2013. Piericidins, novel quorum-sensing inhibitors against *Chromobacterium violaceum* CV026, from *Streptomyces* sp. TOHO-Y209 and TOHO-O348. Open J. Med. Chem. 3, 93–99. https://doi.org/10.4236/ojmc.2013.34012.

Pernezny, K., Collins, J., 1997. Epiphytic populations of *Xanthomonas campestris* pv. *vesicatoria* on pepper: Relationships to host-plant resistance and exposure to copper sprays. Plant Dis. 81, 791–794. https://doi.org/10.1094/PDIS.1997.81.7.791.

Raaijmakers, J.M., De Bruijn, I., De Kock, M.J., 2006. Cyclic lipopeptide production by plant-associated *Pseudomonas* spp.: diversity, activity, biosynthesis, and regulation. Mol. Plant Microbe Interact. 19, 699–710. https://doi.org/10.1094/mpmi-19-0699.

Ramette, A., Frapolli, M., Saux, M.F., Gruffaz, C., Meyer, J., Défago, G., Sutra, L., Moënne-Loccoz, Y., 2011. *Pseudomonas protegens* sp. nov., widespread plant-protecting bacteria producing the biocontrol compounds 2,4-diacetylphloroglucinol and pyoluteorin. Syst. Appl. Microbiol. 34, 180–188. https://doi.org/10.1016/j.syapm.2010.10.005.

Raza, W., Ling, N., Liu, D., Wei, Z., Huang, Q., Shen, Q., 2016. Volatile organic compounds produced by *Pseudomonas fluorescens* WR-1 restrict the growth and virulence traits of *Ralstonia solanacearum*. Microbiol. Res. 192, 103–113. https://doi.org/10.1016/j.micres.2016.05.014.

Richard, D., Tribot, N., Boyer, C., Terville, M., Boyer, K., Javegny, S., Roux-Cuvelier, M., Pruvost, O., Moreau, A., Chabirand, A., Vernière, C., 2017. First report of copper-resistant *Xanthomonas citri* pv. *citri* pathotype causing asiatic citrus canker in Réunion, France. Plant Dis. 503, 101–103. https://doi.org/10.1094/PDIS-09-16-1387-PDN.

Ryan, R.P., An, S.-Q., Allan, J.H., McCarthy, Y., Dow, J.M., 2015. The DSF family of cell–cell signals: an expanding class of bacterial virulence regulators. PLoS Pathog. 11, e1004986. https://doi.org/10.1371/journal.ppat.1004986.

Ryan, R.P., Vorhölter, F., Potnis, N., Jones, J.B., Van Sluys, M., Bogdanove, A.J., Dow, J.M., 2011. Pathogenomics of *Xanthomonas*: understanding bacterium–plant interactions. Nat. Rev. Microbiol. 9 (644–355). https://doi.org/10.1038/nrmicro2558.

Sahu, S.K., Zheng, P., Yao, N., 2018. Niclosamide blocks rice leaf blight by inhibiting biofilm formation of *Xanthomonas oryzae*. Front. Plant Sci. 9, 1–16. https://doi.org/10.3389/fpls.2018.00408.

Shi, L., Li, P., Wang, W., Gao, M., Wu, Z., Song, X., Hu, D., 2015. Antibacterial activity and mechanism of action of sulfone derivatives containing 1,3,4-oxadiazole moieties on rice bacterial leaf blight. Molecules 20, 11660–11675. https://doi.org/10.3390/molecules200711660.

Vasconcellos, Silva, de Oliveira, F., Lopes Santos, A., Oliveira Beranger, L., Torres Cely, A., Simionato, M., Pistori, A., Spago, J., de Mello, F., San Martin, J., Andrade, J., C.J, Andrade, G., 2014. Evaluation of antibiotic activity produced by *Pseudomonas*

aeruginosa LV strain against *Xanthomonas arboricola* pv. *pruni*. Agric. Sci. 5, 71–76. https://doi.org/10.4236/as.2014.51008.

Singh, A., Gupta, R., Tandon, S., Pandey, R., 2017. Thyme oil reduces biofilm formation and impairs virulence of *Xanthomonas oryzae*. Front. Microbiol. 8, 1–16. https://doi.org/10.3389/fmicb.2017.01074.

Sinha, D., Gupta, M.K., Patel, H.K., Ranjan, A., Sonti, R.V., 2013. Cell wall degrading enzyme induced rice innate immune responses are suppressed by the type 3 secretion system effectors XopN, XopQ, XopX and XopZ of *Xanthomonas oryzae*pv.*oryzae*. PLoS One 8, e75867. https://doi.org/10.1371/journal.pone.0075867.

Soboh, F., Khoury, A.E., Zamboni, A.C., Davidson, D., Mittelman, M.W., 1995. Effects of ciprofloxacin and protamine sulfate combinations against catheter-associated *Pseudomonas aeruginosa* biofilms. Antimicrob. Agents Chemother. 39, 1281–1286. https://doi.org/10.1128/AAC.39.6.1281.

Takeuchi, K., Noda, N., Katayose, Y., Mukai, Y., Numa, H., Yamada, K., Someya, N., 2015. Rhizoxin analogs contribute to the biocontrol activity of a newly isolated *Pseudomonas* strain. Mol. Plant Microbe Interact. 28, 333–342. https://doi.org/10.1094/mpmi-09-14-0294-fi.

Tebaldi, N.D., Peters, J., Souza, R.M., Chitarra, L.G., Van der Zouwen, P., Bergervoet, J., Van der Wolf, J., 2010. Detection of *Xanthomonas axonopodis* pv. *phaseoli* in bean seeds by flow cytometry, immunostaining and direct viable counting. Trop. Plant Pathol. 35, 213–222. https://doi.org/10.1590/s1982-56762010000400002.

Vidhyasekaran, P., Kamala, N., Ramanathan, A., Rajappan, K., Paranidharan, V., Velazhahan, R., 2001. Induction of systemic resistance by *Pseudomonas fluorescens* Pf1 against *Xanthomonas oryzae* pv. *oryzae* in rice leaves. Phytoparasitica 29, 155–166. https://doi.org/10.1007/BF02983959.

Williams, P., 2007. Quorum sensing, communication and cross-kingdom signaling in the bacterial world. Microbiology 153, 3923–3938. https://doi.org/10.1099/mic.0.2007/012856-0.

Worthington, R.J., Rogers, S.A., Huigens, R.W., Melander, C., Ritchie, D.F., 2012. Foliar applied small molecule that suppresses biofilm formation and enhances control of copper-resistant *Xanthomonas euvesicatoria* on pepper. Plant Dis. 96, 1638–1644. https://doi.org/10.1094/pdis-02-12-0190-re.

Zhou, L., Wang, X., Zhang, W., Sun, S., He, Y., 2017. Extraction, purification and quantification of diffusible signal factor family quorum-sensing signal molecules in *Xanthomonas oryzae* pv. *oryzae*. Bio-protocol 7, e2190. https://doi.org/10.21769/bioprotoc.2190.

Zhu, H., He, C.C., Chu, Q.H., 2011. Inhibition of quorum sensing in *Chromobacterium violaceum* by pigments extracted from *Auricularia auricular*. Lett. Appl. Microbiol. 52, 269–274. https://doi.org/10.1111/j.1472-765X.2010.02993.x.